Dynamic stiffness analysis of steel-concrete composite beams

Jun Li [*], Qiji Huo, Xiaobin Li, Xiangshao Kong and Weiguo Wu

Key Laboratory of High Performance Ship Technology of Ministry of Education, School of Transportation, Wuhan University of Technology, Wuhan, China

Abstract.   An exact dynamic stiffness method is introduced for investigating the free vibration characteristics of the steel-concrete composite beams consisting of a reinforced concrete slab and a steel beam which are connected by using the stud connectors. The elementary beam theory is used to define the dynamic behaviors of the two beams and the relative transverse deformation of the connectors is included in the formulation. The dynamic stiffness matrix is formulated from the exact analytical solutions of the governing differential equations of the composite beams in undamped free vibration. The application of the derived dynamic stiffness matrix is illustrated to predict the natural frequencies and mode shapes of the steel-concrete composite beams with seven boundary conditions. The present results are compared to the available solutions in the literature whenever possible.

Keywords: steel-concrete composite beams; classical beam theory; free vibration; dynamic stiffness method; analytical models

1. Introduction

Steel-concrete composite beams are widely used in the fields of bridge engineering and building engineering over the past several decades due to some distinguishing features as compared to the steel and concrete counterparts. The steel-concrete composite beam is composed of a reinforced concrete slab and a steel beam which are connected by a set of distributed stud connectors. The concrete slab and the steel beam can slide on the steel-concrete interface. However, this relative sliding is retarded by the stub connectors. On the one hand, this configuration increases the whole stiffness of the composite beam and reduces the overall deformation. On the other hand, this configuration makes the numerical modeling of the behavior of the composite beam more complicated.

The great application of the steel-concrete composite beams in the structural engineering demands a deep understanding of the dynamic characteristics of these structures. A literature survey shows that various aspects of the static behaviors of the steel-concrete composite beams are studied in many research works (Wang 1998, Ranzi and Bradford 2007, Luo *et al.* 2012).

Girhammar and Pan (1993) carried out the exact and approximate dynamic analyses of the composite members with interlayer slip and reached the general closed-form solutions for the

---

*Corresponding author, Professor, E-mail: LJY60023@yahoo.com

displacement functions and the internal forces. On the basis of Bernoulli-Euler beam theory, Adam *et al.* (1997) analyzed the dynamic characteristics of the elastic two-layer beams with interlayer slip using the linear constitutive equation between the horizontal slip and the interlaminar shear force. Biscontin *et al.* (2000) performed the analytical and experimental investigations on the dynamic behaviors of steel-concrete composite beams based on the Bernoulli-Euler beam theory and the same transverse displacement for the steel beam and the concrete slab. Morassi and Rocchetto (2003) presented an experimental investigation on the damage-induced changes in the natural frequencies and mode shapes of the steel-concrete composite beams. In order to accurately describe the dynamic behavior of the steel-concrete composite beam under damaged conditions, Dilena and Morassi (2003) developed an improved analytical model on the basis of the Bernoulli-Euler beam theory. Berczynski and Wroblewski (2005) investigated the free vibrations of the steel-concrete composite beams by means of the analytical solution method, in which both the Bernoulli-Euler beam theory and the Timoshenko beam theory were employed. Based on the Bernoulli-Euler beam theory, Wu *et al.* (2007) investigated the free vibrations of the partial-interaction composite beams with axial force under various classical boundary conditions. Xu and Wu (2007) studied the static, dynamic, and buckling behaviors of the partial-interaction composite beams with the effects of shear deformation and rotary inertia taken into account. Xu and Wu (2008) investigated the free vibration and buckling behaviors of the partial-interaction composite beams using the two-dimensional theory of elasticity and state-space method. Girhammar *et al.* (2009) presented the general solutions of the deflection and internal actions for the free and forced vibrations of the composite Bernoulli-Euler beams with interlayer slip. Dilena and Morassi (2009) adopted a simplified method to model the connections of the steel-concrete composite beams and conducted the vibration analyses based on the Bernoulli-Euler and Timoshenko beam theories. Berczynski and Wroblewski (2010) presented the experimental results of the dynamic characteristics of three steel-concrete composite beams. On the basis of Bernoulli-Euler beam theory, Shen *et al.* (2011) studied the free and forced vibrations of the composite beams with interlayer slip by virtue of state-space method and mode superposition method. Lenci and Clementi (2012) investigated the effects of shear deformation, rotary inertia, axial inertia and interface stiffness on the free vibrations of the composite beams with partial interaction.

This study is a consequence of necessity to establish an exact solution technique that enables the evaluation of the vibration characteristics of the steel-concrete composite beams or frames with various boundary conditions reliably and efficiently. In this paper, the dynamic stiffness method is preferred as a solution technique for analyzing the free vibrations of the steel-concrete composite beam systems. This method is often referred to as an exact method because it is formulated from the exact analytical solutions of the homogeneous governing differential equations. This exact nature makes the dynamic stiffness method exhibit the great advantages when the higher frequencies and better accuracies of the results are demanded. In addition, this method can construct a useful comparator when the traditional finite element or other approximate schemes are employed. To the best of authors' knowledge, the dynamic stiffness method has never been applied to the vibration analyses of the steel-concrete composite beams.

First, the coupled governing equations of motion of the steel-concrete composite beams with shear deformation and rotary inertia excluded are derived by means of the Hamilton's principle. The concrete slab and the steel beam are allowed to slide on their interface and have the same transverse displacement. The reasonable expression is adopted to describe the strain energy of the stud connectors. Then, the theoretical expressions of the dynamic stiffness matrix of the steel-concrete composite beams are derived from the exact general solutions of the homogeneous
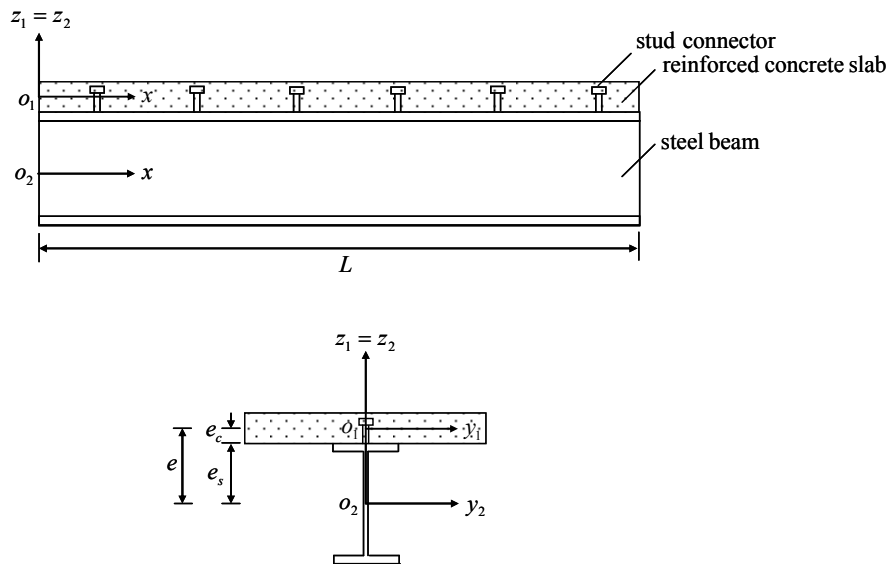
Fig. 1 A steel-concrete composite beam and its cross-section

governing differential equations of motion. Finally, the application of the proposed dynamic stiffness matrix to calculate the modal properties of the steel-concrete composite beams uses the well-known Wittrick-Williams algorithm (Wittrick and Williams 1971). Numerical results of three steel-concrete composite beams with seven different boundary conditions are presented and compared with the available solutions in the literature to illustrate the accuracy and efficiency of the dynamic stiffness approach.

2. Mathematical formulation

Consider a uniform and straight composite beam made of a reinforced concrete slab and a steel beam which are connected by using the stud connectors, as shown in Fig. 1. The concrete slab and the steel beam have the same length L.

The following basic assumptions are made in the analysis.

(1) The concrete slab and the steel beam are linear elastic and isotropic.
(2) Both the transverse shear strains and rotational kinetic energies of the concrete slab and the steel beam are neglected.
(3) The steel-concrete composite beam only vibrates in the oxz_1 plane.
(4) The stud connectors are uniformly distributed and the distance between the two consecutive studs is short enough compared to the beam length. The length of the stud connectors is half of the thickness of the concrete slab.
(5) The concrete slab and the steel beam can slide on the steel-concrete interface and have the same transverse displacement.

The strain energy of the concrete slab is

$$V_1 = \frac{1}{2}\int_0^L E_1 I_1 (w'')^2 dx + \frac{1}{2}\int_0^L E_1 A_1 (u_1')^2 dx \tag{1}$$

where E_1 is the elastic modulus of the concrete slab, A_1 and I_1 are the area and the moment of inertia of the concrete slab cross-section, respectively. $u_1(x, t)$ and $w(x, t)$ are the longitudinal and transverse displacements of a fiber in the middle surface of the concrete slab, respectively. The superscript prime denotes the partial derivative with respect to the coordinate x.

The kinetic energy of the concrete slab is expressed as

$$T_1 = \int_0^L \frac{1}{2} m_1 \left[(\dot{u}_1)^2 + (\dot{w})^2 \right] dx \tag{2}$$

where m_1 is the mass density per unit length of concrete slab. The overdot represents the partial differentiation with respect to the time t.

Similarly, the strain energy V_2 and kinetic energy T_2 of the steel beam are given by

$$V_2 = \frac{1}{2}\int_0^L E_2 I_2 (w'')^2 dx + \frac{1}{2}\int_0^L E_2 A_2 (u_2')^2 dx \tag{3}$$

$$T_2 = \int_0^L \frac{1}{2} m_2 \left[(\dot{u}_2)^2 + (\dot{w})^2 \right] dx \tag{4}$$

where E_2 and m_2 are the elastic modulus and the mass density per unit length of the steel beam, respectively. A_2 and I_2 are the area and the moment of inertia of the steel beam cross-section, respectively. $u_2(x, t)$ and $w(x, t)$ are the longitudinal and transverse displacements of a fiber in the mid-surface of the steel beam, respectively.

The relative sliding between the concrete slab and the steel beam occurs on the steel-concrete interface, which is retarded by the stub connectors. The strain energy of the ith stud connector can be denoted as (Berczynski and Wroblewski 2005)

$$V_{ci} = \frac{1}{2} K \delta_1 \delta_1 + \frac{1}{2} K e_c^2 \zeta_1 \zeta_1 + K e_c \zeta_1 \delta_1 \tag{5}$$

where δ_1 is the difference between the transverse displacements of both ends of the stud connector, which is assumed to be equal to $u_2 - u_1 + w' e_s$, e_s is the distance between the top surface of the steel beam and its centroid; ζ_1 is the rotation angle of the upper end of stud connector, which is equal to the rotation angle of the concrete slab w'; K is the shear stiffness of the stud connector; e_c is the distance between the top surface of the steel beam and the centroid of the concrete slab.

Substituting the expressions of δ_1 and ζ_1 into Eq. (5) yields

$$V_{ci} = \frac{1}{2} K (u_2 - u_1 + w' e)^2 \tag{6}$$

where e is the distance between the centroid of the steel beam and the centroid of the concrete slab, $e = e_s + e_c$.

The stud connectors are assumed to be uniformly distributed and the distance between the two consecutive studs is assumed to be short enough compared to the beam length, which is justified in

the real steel-concrete composite beams. Therefore, the discrete stud connectors can be regarded as a distributed connection along the steel-concrete interface. Under this assumption, the strain energy of the connection can be described as

$$V_c = \int_0^L \frac{1}{2} k \left(u_2 - u_1 + w'e \right)^2 dx \tag{7}$$

where k is the shear stiffness per unit length of the connection, $k = K/d$, in which d is the distance between two consecutive stud connectors.

The governing equations of motion and the corresponding boundary conditions for the coupled transverse and longitudinal vibration of the steel-concrete composite beam are derived by using the Hamilton's principle, which is expressed as

$$\delta \int_{t_1}^{t_2} (T_1 + T_2 - V_1 - V_2 - V_c) dt = 0 \tag{8}$$

$$\delta u_1 = \delta u_2 = \delta w = \delta w' = 0 \quad \text{at} \quad t = t_1, t_2$$

where δ denotes the variation calculus, t_1 and t_2 are two arbitrary time instants.

Substituting Eqs. (1)-(4) and (7) into Eq. (8) and performing the variational operations resulting in the following governing equations of motion of the steel-concrete composite beam

$$- m_1 \ddot{u}_1 + E_1 A_1 u_1'' - k u_1 + k u_2 + k e w' = 0 \tag{9a}$$

$$- m_2 \ddot{u}_2 + k u_1 + E_2 A_2 u_2'' - k u_2 - k e w' = 0 \tag{9b}$$

$$-(m_1 + m_2) \ddot{w} - k e u_1' + k e u_2' - \left(E_1 I_1 + E_2 I_2 \right) w'''' + k e^2 w'' = 0 \tag{9c}$$

The boundary conditions at the beam ends ($x = 0, L$) are given by

$$E_1 A_1 u_1' \; \delta u_1 = 0 \tag{10a}$$

$$E_2 A_2 u_2' \; \delta u_2 = 0 \tag{10b}$$

$$- \left[- k e u_1 + k e u_2 - \left(E_1 I_1 + E_2 I_2 \right) w''' + k e^2 w' \right] \delta w = 0 \tag{10c}$$

$$- \left(E_1 I_1 + E_2 I_2 \right) w'' \, \delta w' = 0 \tag{10d}$$

It is evident from Eqs. (9a)-(9c) that there exists the coupled vibration between the transverse and longitudinal displacements due to the presence of the stud connectors and this coupling is vanished if and only if the connection stiffness k equals zero or the centroid distance e is zero.

3. Derivation of dynamic stiffness matrix

It can be seen that Eqs. (9a)-(9c) are a set of partial differential equations with constant

coefficients, which solutions can be separable in time and space, and the time dependence is harmonic. Thus, the longitudinal displacements u_1 and u_2 as well as the transversal displacement w are assumed as

$$\{u_1(x,t) \quad u_2(x,t) \quad w(x,t)\} = \{U_1(x) \quad U_2(x) \quad W(x)\}e^{i\omega t} \tag{11}$$

where ω is the circular frequency, $U_1(x)$, $U_2(x)$ and $W(x)$ are the amplitudes of the harmonically varying longitudinal displacements and transversal displacement, respectively.

Inserting Eq. (11) into Eqs. (9a)-(9c) and Eqs. (10a)-(10d) yields the following set of ordinary differential equations

$$m_1\omega^2 U_1 + E_1 A_1 U_1'' - kU_1 + kU_2 + keW' = 0 \tag{12a}$$

$$m_2\omega^2 U_2 + kU_1 + E_2 A_2 U_2'' - kU_2 - keW' = 0 \tag{12b}$$

$$(m_1 + m_2)\omega^2 W - keU_1' + keU_2' - (E_1 I_1 + E_2 I_2)W'''' + ke^2 W'' = 0 \tag{12c}$$

and the corresponding boundary conditions

$$E_1 A_1 U_1' \, \delta U_1 = 0 \tag{13a}$$

$$E_2 A_2 U_2' \, \delta U_2 = 0 \tag{13b}$$

$$\left[keU_1 - keU_2 + (E_1 I_1 + E_2 I_2)W''' - ke^2 W'\right]\delta W = 0 \tag{13c}$$

$$-(E_1 I_1 + E_2 I_2)W''\delta W' = 0 \tag{13d}$$

The amplitude functions $U_1(x)$, $U_2(x)$ and $W(x)$ of the longitudinal displacements and transversal displacement can be considered as follows

$$\{U_1(x) \quad U_2(x) \quad W(x)\} = \{\tilde{A} \quad \tilde{B} \quad \tilde{C}\}e^{\kappa x} \tag{14}$$

Introducing Eq. (14) into Eqs. (12a)-(12c) obtains the algebraic eigenvalue equations, which have nontrivial solutions when the determinant of the coefficient matrix of $\tilde{A}$, $\tilde{B}$ and $\tilde{C}$ vanishes. Let the determinant equal to zero results in the characteristics equation, which is an eighth-order polynomial equation in κ

$$\eta_4\kappa^8 + \eta_3\kappa^6 + \eta_2\kappa^4 + \eta_1\kappa^2 + \eta_0 = 0 \tag{15}$$

where

$$\eta_4 = -E_1 A_1 E_2 A_2 (E_1 I_1 + E_2 I_2)$$

$$\eta_3 = E_2 A_2 (E_1 I_1 + E_2 I_2)(k - m_1\omega^2) + E_1 A_1 (E_2 A_2 e^2 k + (E_1 I_1 + E_2 I_2)(k - m_2\omega^2))$$

$$\eta_2 = \omega^2 (E_2 A_2 e^2 km_1 + E_1 A_1 (e^2 km_2 + E_2 A_2 (m_1 + m_2)) + (E_1 I_1 + E_2 I_2)(k(m_1 + m_2) - m_1 m_2\omega^2))$$

$$\eta_1 = \omega^2 (e^2 km_1 m_2\omega^2 + E_2 A_2 (m_1 + m_2)(-k + m_1\omega^2) + E_1 A_1 (m_1 + m_2)(-k + m_2\omega^2))$$

$$\eta_0 = (m_1 + m_2)\omega^4(-k(m_1 + m_2) + m_1 m_2 \omega^2)$$

Let $\chi = \kappa^2$ and substituting it into Eq. (15) yields a fourth-order polynomial equation

$$\chi^4 + a_1\chi^3 + a_2\chi^2 + a_3\chi + a_4 = 0 \tag{16}$$

where

$$a_1 = \eta_3/\eta_4 \qquad a_2 = \eta_2/\eta_4 \qquad a_3 = \eta_1/\eta_4 \qquad a_4 = \eta_0/\eta_4$$

A closed-form solution to Eq. (16) can be found as follows. Eq. (16) can be factored into the product of two quadratic polynomial equations

$$(\chi^2 + p_1\chi + q_1)(\chi^2 + p_2\chi + q_2) = 0 \tag{17}$$

where

$$\begin{Bmatrix} p_1 \\ p_2 \end{Bmatrix} = \frac{1}{2}\left[a_1 \pm \sqrt{a_1^2 - 4a_2 + 4\lambda_1} \right] \qquad \begin{Bmatrix} q_1 \\ q_2 \end{Bmatrix} = \frac{1}{2}\left[\lambda_1 \pm \frac{a_1\lambda_1 - 2a_3}{\sqrt{a_1^2 - 4a_2 + 4\lambda_1}} \right]$$

The parameter λ_1 is a real root of the following cubic equation

$$\lambda^3 - a_2\lambda^2 + (a_1a_3 - 4a_4)\lambda + (4a_2a_4 - a_3^2 - a_1^2 a_4) = 0 \tag{18}$$

The four roots of Eq. (16) follow

$$\begin{Bmatrix} \chi_1 \\ \chi_2 \end{Bmatrix} = -\frac{p_1}{2} \pm \sqrt{\frac{p_1^2}{4} - q_1} \qquad \begin{Bmatrix} \chi_3 \\ \chi_4 \end{Bmatrix} = -\frac{p_2}{2} \pm \sqrt{\frac{p_2^2}{4} - q_2} \tag{19}$$

Then the general solutions to Eqs. (12a)-(12c) can be written as

$$U_1(x) = \overline{A}_1 e^{\kappa_1 x} + \overline{A}_2 e^{-\kappa_1 x} + \overline{A}_3 e^{\kappa_2 x} + \overline{A}_4 e^{-\kappa_2 x} + \overline{A}_5 e^{\kappa_3 x} + \overline{A}_6 e^{-\kappa_3 x} + \overline{A}_7 e^{\kappa_4 x} + \overline{A}_8 e^{-\kappa_4 x}$$
$$= \sum_{j=1}^{4} (\overline{A}_{2j-1} e^{\kappa_j x} + \overline{A}_{2j} e^{-\kappa_j x}) \tag{20a}$$

$$U_2(x) = \overline{B}_1 e^{\kappa_1 x} + \overline{B}_2 e^{-\kappa_1 x} + \overline{B}_3 e^{\kappa_2 x} + \overline{B}_4 e^{-\kappa_2 x} + \overline{B}_5 e^{\kappa_3 x} + \overline{B}_6 e^{-\kappa_3 x} + \overline{B}_7 e^{\kappa_4 x} + \overline{B}_8 e^{-\kappa_4 x}$$
$$= \sum_{j=1}^{4} (\overline{B}_{2j-1} e^{\kappa_j x} + \overline{B}_{2j} e^{-\kappa_j x}) \tag{20b}$$

$$W(x) = \overline{C}_1 e^{\kappa_1 x} + \overline{C}_2 e^{-\kappa_1 x} + \overline{C}_3 e^{\kappa_2 x} + \overline{C}_4 e^{-\kappa_2 x} + \overline{C}_5 e^{\kappa_3 x} + \overline{C}_6 e^{-\kappa_3 x} + \overline{C}_7 e^{\kappa_4 x} + \overline{C}_8 e^{-\kappa_4 x}$$
$$= \sum_{j=1}^{4} (\overline{C}_{2j-1} e^{\kappa_j x} + \overline{C}_{2j} e^{-\kappa_j x}) \tag{20c}$$

where $\overline{A}_{2j-1}(\overline{A}_{2j})$, $\overline{B}_{2j-1}(\overline{B}_{2j})$ and $\overline{C}_{2j-1}(\overline{C}_{2j})$ are three sets of undetermined constants, $\kappa_j = \sqrt{\chi_j}$ $(j = 1-4)$. In the solution of Eq. (16), if any of the χ_j's are zero or are repeated, the solutions to Eqs. (12a)-(12c) will be revised using the well-known methods for the ordinary differential equations with constant coefficients, for those particular values of χ_j.

Substituting Eqs. (20a)-(20c) into Eqs. (12a)-(12b) obtains the following relations among the three sets of unknown constants

$$\overline{A}_{2j-1} = t_j \overline{C}_{2j-1} \qquad \overline{A}_{2j} = -t_j \overline{C}_{2j} \tag{21a}$$

$$\overline{B}_{2j-1} = \bar{t}_j \overline{C}_{2j-1} \qquad \overline{B}_{2j} = -\bar{t}_j \overline{C}_{2j} \tag{21b}$$

where

$$t_j = ek\kappa_j (E_2 A_2 \kappa_j^2 + m_2 \omega^2) / \Delta \qquad \bar{t}_j = -ek\kappa_j (E_1 A_1 \kappa_j^2 + m_1 \omega^2) / \Delta$$

$$\Delta = k(m_1 + m_2)\omega^2 - m_1 m_2 \omega^4 + E_2 A_2 \kappa_j^2 (k - m_1 \omega^2) + E_1 A_1 \kappa_j^2 (k - E_2 A_2 \kappa_j^2 - m_2 \omega^2)$$

Substituting Eqs. (20a)-(20c) into Eqs. (13a)-(13d) and adopting the sign convention shown in Fig. 2, the expressions for the normal forces $N_1(x)$ and $N_2(x)$, shear force $S(x)$ and bending moment $M(x)$ can be written in terms of the constants $\overline{C}_{2j-1}(\overline{C}_{2j})$

$$N_1(x) = E_1 A_1 U_1' = \sum_{j=1}^{4} E_1 A_1 t_j \kappa_j \left(\overline{C}_{2j-1} e^{\kappa_j x} + \overline{C}_{2j} e^{-\kappa_j x} \right) \tag{22a}$$

$$N_2(x) = E_2 A_2 U_2' = \sum_{j=1}^{4} E_2 A_2 \bar{t}_j \kappa_j \left(\overline{C}_{2j-1} e^{\kappa_j x} + \overline{C}_{2j} e^{-\kappa_j x} \right) \tag{22b}$$

$$S(x) = keU_1 - keU_2 + (E_1 I_1 + E_2 I_2)W''' - ke^2 W'$$
$$= \sum_{j=1}^{4} \left[ket_j - ke\bar{t}_j + (E_1 I_1 + E_2 I_2)\kappa_j^3 - ke^2 \kappa_j \right] \left(\overline{C}_{2j-1} e^{\kappa_j x} - \overline{C}_{2j} e^{-\kappa_j x} \right) \tag{22c}$$

$$M(x) = -(E_1 I_1 + E_2 I_2)W'' = \sum_{j=1}^{4} -(E_1 I_1 + E_2 I_2)\kappa_j^2 \left(\overline{C}_{2j-1} e^{\kappa_j x} + \overline{C}_{2j} e^{-\kappa_j x} \right) \tag{22d}$$
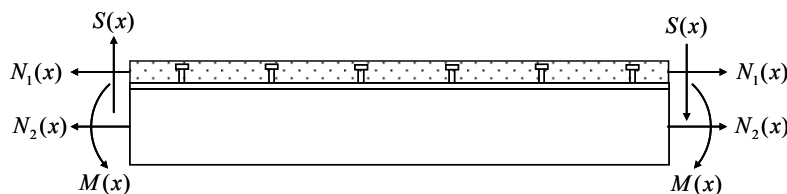

Fig. 2 Sign convention for positive normal forces $N_1(x)$ and $N_2(x)$, shear force $S(x)$ and bending moment $M(x)$
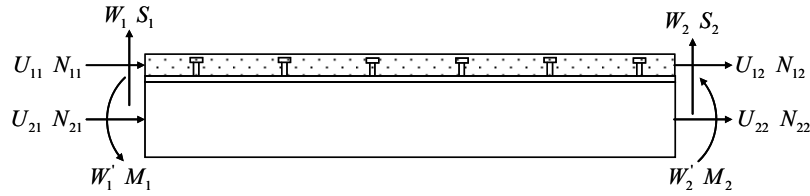
Fig. 3 Boundary conditions for generalized displacements and forces

With reference to Fig. 3, the end conditions for the generalized displacements and generalized forces of the steel-concrete composite beam are, respectively

$$x = 0: \quad U_1 = U_{11} \quad U_2 = U_{21} \quad W = W_1 \quad W' = W_1' \tag{23a}$$

$$x = L: \quad U_1 = U_{12} \quad U_2 = U_{22} \quad W = W_2 \quad W' = W_2' \tag{23b}$$

$$x = 0: \quad N_1 = -N_{11} \quad N_2 = -N_{21} \quad S = S_1 \quad M = M_1 \tag{23c}$$

$$x = L \quad N_1 = N_{12} \quad N_2 = N_{22} \quad S = -S_2 \quad M = -M_2 \tag{23d}$$

Introducing Eqs. (23a) and (23c) into Eqs. (20a)-(20c), the nodal displacements at the beam ends can be expressed in terms of the constants $\overline{C}_{2j-1}(\overline{C}_{2j})$ as

$$\{D\} = [R]\{\overline{C}\} \tag{24}$$

where $\{D\}$ is the nodal displacement vector defined by

$$\{D\} = \{U_{11} \quad U_{21} \quad W_1 \quad W_1' \quad U_{12} \quad U_{22} \quad W_2 \quad W_2'\}^T$$

$$\{\overline{C}\} = \{\overline{C}_1 \quad \overline{C}_3 \quad \overline{C}_5 \quad \overline{C}_7 \quad \overline{C}_2 \quad \overline{C}_4 \quad \overline{C}_6 \quad \overline{C}_8\}^T$$

$$[R] = \begin{bmatrix} t_1 & t_2 & t_3 & t_4 & -t_1 & -t_2 & -t_3 & -t_4 \\ \bar{t}_1 & \bar{t}_2 & \bar{t}_3 & \bar{t}_4 & -\bar{t}_1 & -\bar{t}_2 & -\bar{t}_3 & -\bar{t}_4 \\ 1 & 1 & 1 & 1 & 1 & 1 & 1 & 1 \\ \kappa_1 & \kappa_2 & \kappa_3 & \kappa_4 & -\kappa_1 & -\kappa_2 & -\kappa_3 & -\kappa_4 \\ t_1 e^{\kappa_1 L} & t_2 e^{\kappa_2 L} & t_3 e^{\kappa_3 L} & t_4 e^{\kappa_4 L} & -t_1 e^{-\kappa_1 L} & -t_2 e^{-\kappa_2 L} & -t_3 e^{-\kappa_3 L} & -t_4 e^{-\kappa_4 L} \\ \bar{t}_1 e^{\kappa_1 L} & \bar{t}_2 e^{\kappa_2 L} & \bar{t}_3 e^{\kappa_3 L} & \bar{t}_4 e^{\kappa_4 L} & -\bar{t}_1 e^{-\kappa_1 L} & -\bar{t}_2 e^{-\kappa_2 L} & -\bar{t}_3 e^{-\kappa_3 L} & -\bar{t}_4 e^{-\kappa_4 L} \\ e^{\kappa_1 L} & e^{\kappa_2 L} & e^{\kappa_3 L} & e^{\kappa_4 L} & e^{-\kappa_1 L} & e^{-\kappa_2 L} & e^{-\kappa_3 L} & e^{-\kappa_4 L} \\ \kappa_1 e^{\kappa_1 L} & \kappa_2 e^{\kappa_2 L} & \kappa_3 e^{\kappa_3 L} & \kappa_4 e^{\kappa_4 L} & -\kappa_1 e^{-\kappa_1 L} & -\kappa_2 e^{-\kappa_2 L} & -\kappa_3 e^{-\kappa_3 L} & -\kappa_4 e^{-\kappa_4 L} \end{bmatrix}$$

Substituting Eqs. (23b) and (23d) into Eqs. (22a)-(22d), the nodal forces at the beam ends

corresponding to the nodal displacements also can be expressed in terms of the coefficients $\overline{C}_{2j-1}(\overline{C}_{2j})$ as

$$\{F\} = [H]\{\overline{C}\} \tag{25}$$

where $\{F\}$ is the nodal force vector defined by

$$\{F\} = \{N_{11} \quad N_{21} \quad S_1 \quad M_1 \quad N_{12} \quad N_{22} \quad S_2 \quad M_2\}^T$$

$$[H] = \begin{bmatrix}
-\hat{t}_1 & -\hat{t}_2 & -\hat{t}_3 & -\hat{t}_4 & -\hat{t}_1 & -\hat{t}_2 & -\hat{t}_3 & -\hat{t}_4 \\
-\tilde{t}_1 & -\tilde{t}_2 & -\tilde{t}_3 & -\tilde{t}_4 & -\tilde{t}_1 & -\tilde{t}_2 & -\tilde{t}_3 & -\tilde{t}_4 \\
\bar{\bar{t}}_1 & \bar{\bar{t}}_2 & \bar{\bar{t}}_3 & \bar{\bar{t}}_4 & -\bar{\bar{t}}_1 & -\bar{\bar{t}}_2 & -\bar{\bar{t}}_3 & -\bar{\bar{t}}_4 \\
\hat{\hat{t}}_1 & \hat{\hat{t}}_2 & \hat{\hat{t}}_3 & \hat{\hat{t}}_4 & \hat{\hat{t}}_1 & \hat{\hat{t}}_2 & \hat{\hat{t}}_3 & \hat{\hat{t}}_4 \\
\hat{t}_1 e^{\kappa_1 L} & \hat{t}_2 e^{\kappa_2 L} & \hat{t}_3 e^{\kappa_3 L} & \hat{t}_4 e^{\kappa_4 L} & \hat{t}_1 e^{-\kappa_1 L} & \hat{t}_2 e^{-\kappa_2 L} & \hat{t}_3 e^{-\kappa_3 L} & \hat{t}_4 e^{-\kappa_4 L} \\
\tilde{t}_1 e^{\kappa_1 L} & \tilde{t}_2 e^{\kappa_2 L} & \tilde{t}_3 e^{\kappa_3 L} & \tilde{t}_4 e^{\kappa_4 L} & \tilde{t}_1 e^{-\kappa_1 L} & \tilde{t}_2 e^{-\kappa_2 L} & \tilde{t}_3 e^{-\kappa_3 L} & \tilde{t}_4 e^{-\kappa_4 L} \\
-\bar{\bar{t}}_1 e^{\kappa_1 L} & -\bar{\bar{t}}_2 e^{\kappa_2 L} & -\bar{\bar{t}}_3 e^{\kappa_3 L} & -\bar{\bar{t}}_4 e^{\kappa_4 L} & \bar{\bar{t}}_1 e^{-\kappa_1 L} & \bar{\bar{t}}_2 e^{-\kappa_2 L} & \bar{\bar{t}}_3 e^{-\kappa_3 L} & \bar{\bar{t}}_4 e^{-\kappa_4 L} \\
-\hat{\hat{t}}_1 e^{\kappa_1 L} & -\hat{\hat{t}}_2 e^{\kappa_2 L} & -\hat{\hat{t}}_3 e^{\kappa_3 L} & -\hat{\hat{t}}_4 e^{\kappa_4 L} & -\hat{\hat{t}}_1 e^{-\kappa_1 L} & -\hat{\hat{t}}_2 e^{-\kappa_2 L} & -\hat{\hat{t}}_3 e^{-\kappa_3 L} & -\hat{\hat{t}}_4 e^{-\kappa_4 L}
\end{bmatrix}$$

in which

$$\hat{t}_j = E_1 A_1 t_j \kappa_j \qquad \tilde{t}_j = E_2 A_2 \bar{t}_j \kappa_j \qquad \bar{\bar{t}}_j = ket_j - ke\bar{t}_j + (E_1 I_1 + E_2 I_2)\kappa_j^3 - ke^2 \kappa_j$$

$$\hat{\hat{t}}_j = -(E_1 I_1 + E_2 I_2)\kappa_j^2 \qquad (j = 1-4)$$

Combining Eqs. (24) and (25) and eliminating the constant vector $\{\overline{C}\}$ produces the relation between the nodal force vector $\{F\}$ and the nodal displacement vector $\{D\}$

$$\{F\} = [H][R]^{-1}\{D\} = [\overline{K}]\{D\} \tag{26}$$

where $[\overline{K}] = [H][R]^{-1}$ is called the exact element dynamic stiffness matrix. Note that the roots of Eq. (16) can be real or complex depending on the coefficients of Eq. (16), and as a consequence, the elements of matrices $[R]$ and $[H]$ can be complex. Therefore, the matrix inversion and multiplication involved in Eq. (26) must be performed using complex arithmetic. However, the resulting dynamic stiffness matrix $[K]$ will be symmetric and real. It may be mentioned that the analytical expressions for the elements of the dynamic stiffness matrix can be derived using the symbol manipulation software Mathematica (Wolfram 1991), which can lead to substantial savings in computational cost. However, these expressions are too lengthy to be listed in the paper.

The derived element dynamic stiffness matrix can be directly used to compute the natural frequencies and mode shapes of the individual steel-concrete composite beam. If an assembly of the steel-concrete composite beams is under consideration, the global dynamic stiffness matrix for the entire beam system can be assembled from each element dynamic stiffness matrix in a completely similar way to that used for the traditional finite element method. The well-known Wittrick-Williams algorithm (Wittrick and Williams 1971, Banerjee 1997) is chosen in this paper to calculate the natural frequencies of the steel-concrete composite beams. The algorithm is reliable and efficient because it finds the total number of natural frequencies below an arbitrarily

given trial value instead of directly calculating the natural frequencies. In this way the upper and lower bounds are established for each required natural frequency, and then the classical bisection method can be used to determine the natural frequencies to any required accuracy. Due to the extensive discussions on the use of the algorithm in the literature, the detailed process is not repeated here. The mode shapes corresponding to the natural frequencies can be found in the usual way by making an arbitrary assumption about one unknown variable of the steel-concrete composite beam assembly and then calculating the remaining variables in terms of the arbitrarily chosen one.

4. Results and discussion

In order to illustrate the application of the dynamic stiffness matrix derived in the preceding sections, numerical calculations are performed on three steel-concrete composite beams. Four classical boundary conditions at the ends of each beam are considered, i.e., clamped end, hinged end 1, hinged end 2 and free end.

For the clamped end (C): $U_1 = U_2 = W = W' = 0$
For the hinged end 1 (H1): $U_1 = U_2 = W = M = 0$
For the hinged end 2 (H2): $N_1 = N_2 = W = M = 0$
For the free end (F): $N_1 = N_2 = S = M = 0$

A total of seven boundary conditions, i.e., C-C, C-H1, C-H2, F-F, C-F, H1-H1 and H2-H2 are considered for each beam.

The composite beams under consideration are similar to those studied in references (Biscontin *et al.* 2000, Morassi and Rocchetto 2003, Dilena and Morassi 2003). However, a brief description of the beams is given for the sake of completeness. Each composite beam is composed of a steel beam made of a Fe430 steel section bar of IPE 140 series and a concrete slab with 0.06m thick and 0.5 m wide, which are connected through a series of Fe430 steel studs. The geometric and material properties of the steel beam are equal to their nominal values, i.e., elastic modulus $E_2 = 2.1 \times 10^{11}$ N/m^2, mass density per unit length $m_2 = 12.9$ kg/m, cross-sectional area $A_2 = 1.64 \times 10^{-3}$ m^2, and moment of inertia $I_2 = 5.41 \times 10^{-6}$ m^4. As for the concrete slab, the cross-sectional area is $A_1 = 3 \times 10^{-2}$ m^2, and moment of inertia is $I_1 = 9 \times 10^{-6}$ m^4. The distance between the top surface of the steel beam and the centroid of the concrete slab is $e_c = 0.03$ m, and the distance between the top surface of the steel beam and its centroid is $e_s = 0.07$ m. Both the length of the steel beam and concrete slab are $L = 3.5$ m.

The elastic modulus E_1 and mass density per unit length m_1 of the concrete slab as well as the shear stiffness K of the stud connector and the distance d between two consecutive stud connectors have different values for the three composite beams under investigation.

For the composite beam A:
$E_1 = 4.539 \times 10^{10}$ N/m^2, $m_1 = 78.07$ kg/m, $K = 2.858 \times 10^8$ N/m, $d = 0.21875$ m

For the composite beam B:
$E_1 = 4.229 \times 10^{10}$ N/m^2, $m_1 = 73.19$ kg/m, $K = 2.367 \times 10^8$ N/m, $d = 0.21875$ m

For the composite beam C:
$E_1 = 4.098 \times 10^{10}$ N/m^2, $m_1 = 75.84$ kg/m, $K = 2.055 \times 10^8$ N/m, $d = 0.15217$ m

A detailed numerical investigation is performed on the three steel-concrete composite beams with seven different boundary conditions. The natural frequencies of the composite beams are evaluated by virtue of the exact dynamic stiffness matrix established in this paper. Each beam is idealized with only one element throughout this section. The first ten natural frequencies are determined for each beam and each boundary condition. The numerical results are shown in Tables 1-3, together with some solutions available in the literature. For the composite beam A with F-F boundary condition, the natural frequencies for the first eight bending vibration modes and for the first two longitudinal vibration modes obtained in reference (Biscontin *et al.* 2000) by using the analytical method and experimental technique are displayed in Table 1. It may be mentioned that the rigid vibration modes are omitted for the composite beams with F-F boundary condition and the values with superscript asterisk denote the natural frequencies corresponding to the longitudinal vibration modes. The present mathematical model is similar to the one used in reference (Biscontin *et al.* 2000), but there is a small difference in describing the strain energy of the stud connectors. For the composite beams B and C with F-F boundary condition, the experiment results for the first seven bending vibration frequencies and for the first two longitudinal vibration frequencies acquired in reference (Morassi and Rocchetto 2003) are presented in Tables 2-3, respectively. In addition, the first seven bending vibration frequencies gained in reference (Dilena and Morassi 2003) by means of the analytical method are also given in Tables 2-3. The definition of the strain energy of the stud connectors in reference (Dilena and Morassi 2003) is the same as the one in reference (Biscontin *et al.* 2000) and the analytical results cited from reference (Dilena and Morassi 2003) are based on the assumptions that the relative transverse displacement can occur between the concrete slab and the steel beam as well as the axial stiffness of the stud connectors is infinity.

It can be seen from the results presented in Tables 1-3 that the natural frequencies of the composite beams are sensitive to the variations of the boundary condition. The variation of the natural frequency with the boundary condition can be observed from Tables 1-3. The natural frequencies of the composite beams with F-F boundary condition are the highest and the composite beams with C-F boundary condition have the lowest natural frequencies. The natural

Table 1 Natural frequencies (in Hz) for the composite beam A

Mode no.	C-C	C-H1	C-H2	F-F			C-F	H1-H1	H2-H2
				Present	Morassi and Rocchetto (2003)	Biscontin *et al.* (2000)			
1	53.87	47.28	42.33	59.62	59.625	59.625	9.71	41.92	35.43
2	135.51	119.89	116.62	148.05	148.038	133.875	55.41	106.42	95.11
3	248.90	224.18	222.25	265.54	265.496	235.250	141.88	201.77	198.91
4	392.25	358.87	357.29	410.36	410.268	345.000	257.12	327.75	309.86
5	566.32	524.40	441.20	584.29	584.174	459.000	309.20	484.72	345.69
6	617.54	617.54	524.72	617.83[*]	617.750[*]	617.750[*]	401.38	617.54	483.75
7	771.85	721.41	721.32	789.13	788.895	578.250	575.44	673.20	673.13
8	1009.45	950.50	950.21	1025.44	1025.059	706.750	780.54	893.77	758.29
9	1229.44	1212.08	970.67	1229.19[*]	1229.303[*]	1233.625[*]	924.47	1146.82	893.95
10	1279.54	1229.44	1212.09	1293.52	1292.848	853.000	1017.46	1229.44	1146.71

Table 2 Natural frequencies (in Hz) for the composite beam B

Mode no.	C-C	C-H1	C-H2	F-F			C-F	H1-H1	H2-H2
				Present	Dilena and Morassi (2003)	Morassi and Rocchetto (2003)			
1	53.91	46.80	42.23	60.27	60.56	60.56	9.86	41.08	35.03
2	135.27	118.88	116.22	148.16	137.99	143.68	55.68	104.74	95.30
3	248.80	223.24	221.77	265.13	246.98	241.90	141.87	200.02	197.82
4	393.04	358.70	357.56	410.23	387.01	345.68	256.87	326.67	310.37
5	568.94	525.91	437.95	585.57	559.30	455.88	309.02	485.17	340.81
6	616.95	616.95	526.11	617.29*	617.06*	617.06*	401.73	616.95	484.48
7	777.20	725.50	725.43	792.89	764.59	566.88	577.40	676.06	676.00
8	1018.40	958.03	957.59	1032.64	1003.27	688.88	785.11	899.90	749.98
9	1226.93	1223.84	964.60	1226.75*	N/A	1225.94*	923.12	1157.04	899.99
10	1292.88	1226.94	1223.85	1304.14	N/A	N/A	1025.50	1226.93	1156.97

For the composite beam B with F-F boundary condition, Table 2 illustrates that the first seven bending natural frequencies predicted by the present formulation agree well with the analytical results in reference (Dilena and Morassi 2003). The relative errors for the first seven bending natural frequencies are 0.5%, 7.4%, 7.3%, 6.0%, 4.7%, 3.7% and 2.9%, which may be attributed to the different mathematical models used. It can also be found that as the bending mode number increases, the differences between the present results and the experimental values in reference (Morassi and Rocchetto 2003) increase. However, the natural frequencies of the first two longitudinal vibration modes predicted by the present formulation are virtually coincident with the experimental data in reference (Morassi and Rocchetto 2003). With the exception of the fundamental mode, the present model overestimates the natural frequencies as compared with the experiment values.

Table 3 Natural frequencies (in Hz) for the composite beam C

Mode no.	C-C	C-H1	C-H2	F-F			C-F	H1-H1	H2-H2
				Present	Dilena and Morassi (2003)	Morassi and Rocchetto (2003)			
1	54.20	47.76	42.39	59.81	62.03	62.03	9.72	42.49	35.34
2	136.44	121.00	117.36	148.95	139.50	146.53	55.69	107.70	95.70
3	250.49	225.93	223.72	267.33	248.29	246.59	142.78	203.67	200.35
4	394.41	361.17	359.33	412.94	387.30	351.25	258.80	330.20	312.84
5	568.92	527.14	438.54	586.83	557.43	460.25	300.64	487.61	350.49
6	600.16	600.16	527.43	601.07*	N/A	600.31*	403.74	600.16	486.43
7	774.74	724.45	724.32	792.62	759.72	568.63	578.30	676.40	676.28
8	1012.52	953.72	946.61	1029.14	994.46	677.50	783.71	897.14	749.23
9	1193.11	1193.11	954.55	1193.00*	N/A	1189.60*	897.91	1150.30	897.32
10	1282.69	1215.40	1215.40	1297.31	N/A	N/A	1020.85	1193.11	1150.12

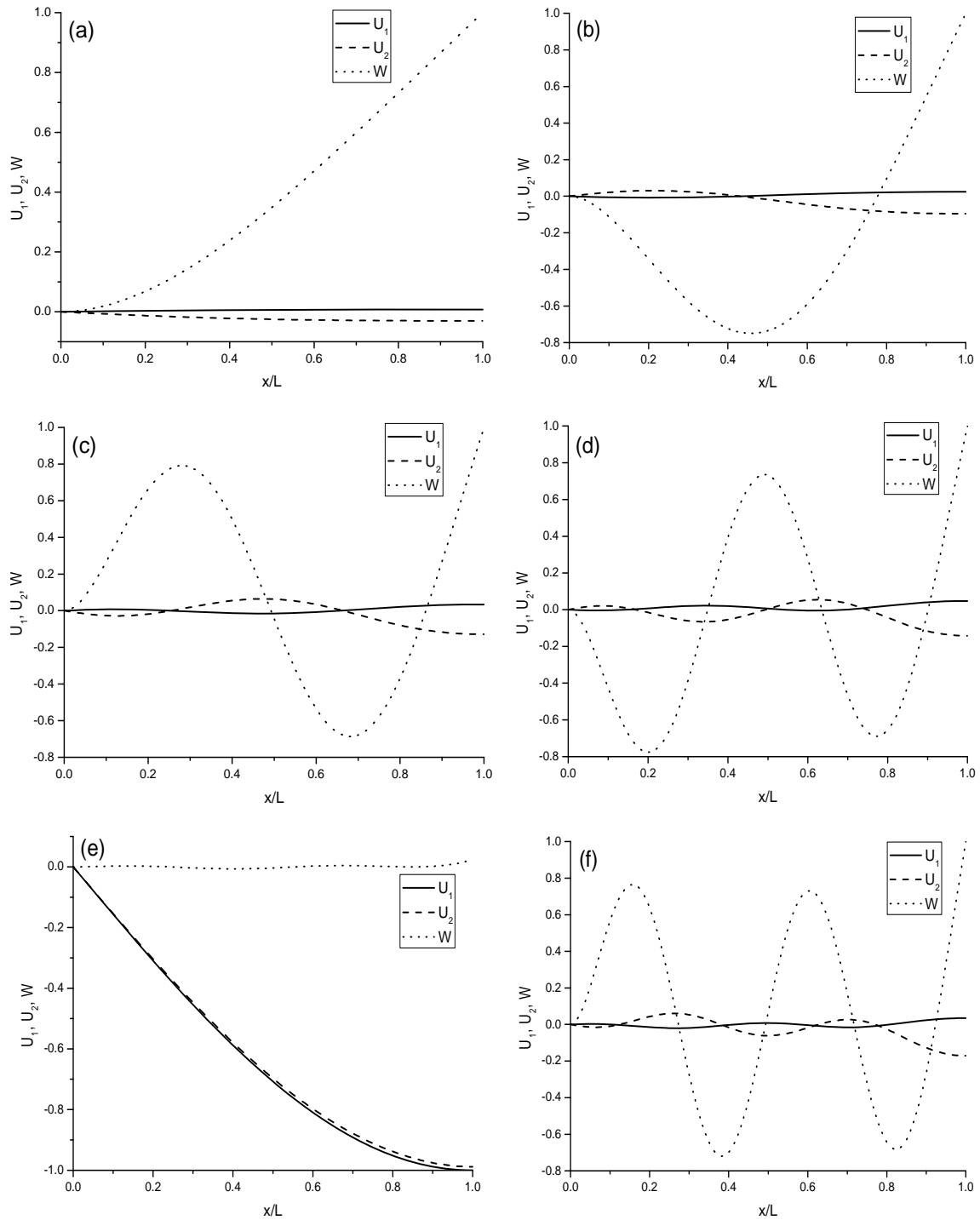*Jun Li, Qiji Huo, Xiaobin Li, Xiangshao Kong and Weiguo Wu*

Fig. 4 First ten normal mode shapes of the composite beam A with C-F boundary condition: (a) mode 1; (b) mode 2; (c) mode 3; (d) mode 4; (e) mode 5; (f) mode 6; (g) mode 7; (h) mode 8; (i) mode 9; (j) mode 10
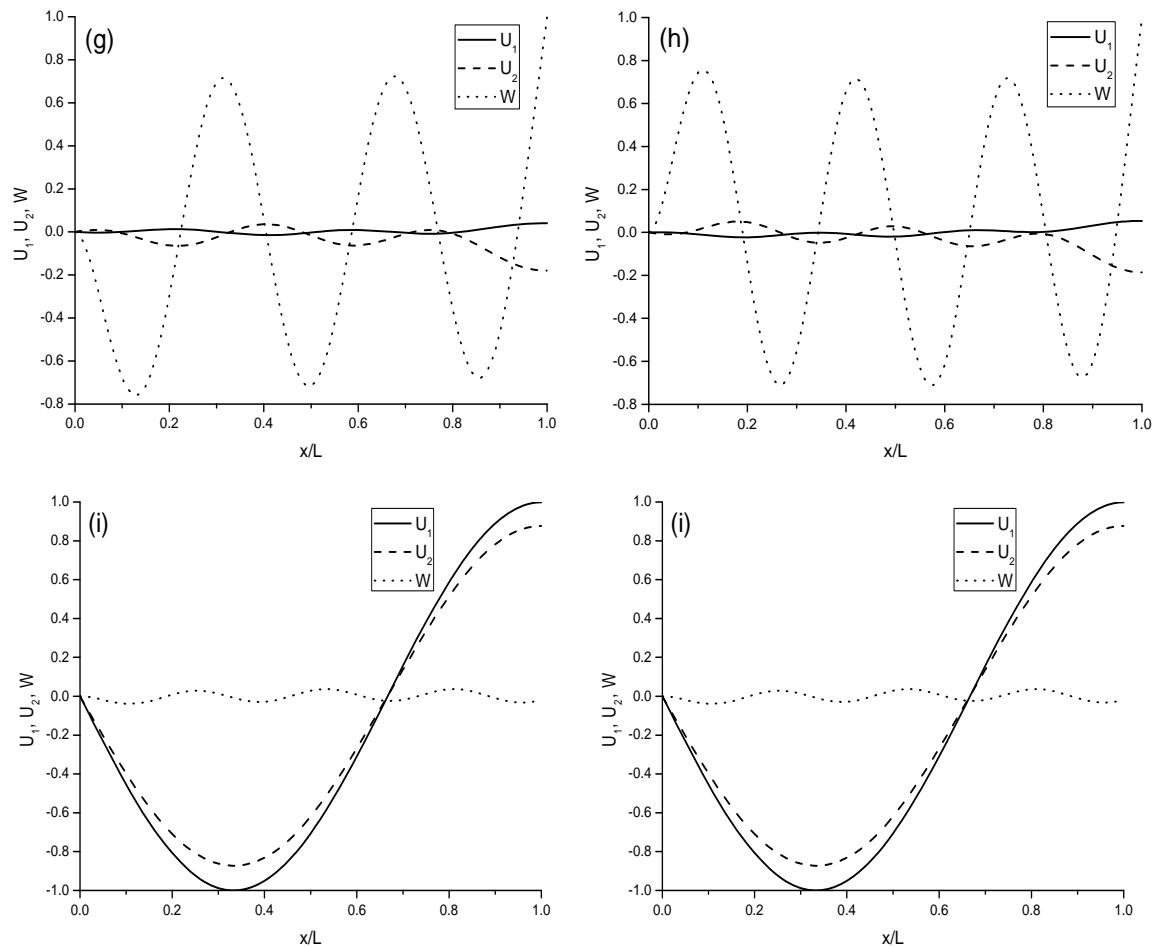
Fig. 4 Continued

frequencies of the composite beams with C-H1 and H1-H1 boundary conditions are larger than those of the composite beams with C-H2 and H2-H2 boundary conditions, respectively.

For the composite beam A with F-F boundary condition, it can be seen from Table 1 that the first ten natural frequencies obtained by the present formulation are in excellent agreement with the analytical results in reference (Biscontin *et al.* 2000). However, a comparison between the present results and the experimental values in reference (Biscontin *et al.* 2000) shows that a good agreement is observed for the lower natural frequencies and a fairly large difference can be found for the higher natural frequencies. The relative errors for the first eight bending natural frequencies are 0, 10.6%, 12.9%, 18.9%, 27.3%, 36.5%, 45.1% and 51.6%. The present results are consistently larger than the experimental values and the relative errors increase with the increase of the mode number, which may implicate that the shear deformation and rotary inertia will play an important role for the higher bending natural frequencies.

For the composite beam C with F-F boundary condition, similar conclusions to the composite beam B can be drawn.

The first ten normal mode shapes of the steel-concrete composite beam A with C-F boundary condition are computed and plotted in Figs. 4(a)-(j). It can be seen from Figs. 4(a)-(j) that of the ten natural frequencies under investigation the fifth and ninth natural frequencies are corresponding to the longitudinal vibration modes. Another observation is that the bending vibration is coupled with the longitudinal vibration, which is due to the nonzero shear stiffness of the stud connectors or the nonzero distance between the centroid of the steel beam and the centroid of the concrete slab. In addition, it can also be found from Figs. 4(a)-(j) that the differences between the longitudinal displacement components of the vibration modes in the steel beam and concrete slab are obvious.

5. Conclusions

This paper presents a dynamic stiffness formulation for investigating the free vibration of the steel-concrete composite beams with the effect of relative longitudinal deformation between the concrete slab and the steel beam included. The dynamic stiffness matrix is formulated from the closed-from general solutions of the homogeneous governing differential equations of the steel-concrete composite beams. The dynamic stiffness method is illustrated by its application to compute the natural frequencies and mode shapes of the composite beams using the Wittrick-Williams algorithm. Numerical results of three steel-concrete composite beams with seven different boundary conditions are presented and compared to the available solutions in the literature. For the particular composite beams under consideration, the F-F composite beams have the highest natural frequencies and the C-F composite beams have the lowest ones. A comparison between the present results and the experimental values shows that an excellent agreement is observed for the first two longitudinal vibration natural frequencies, a good agreement for the lower bending vibration natural frequencies and a fairly large difference for the higher ones, the errors may be ascribed to the ignorance of the shear deformation and rotary inertia in the present formulation. It is anticipated that the dynamic stiffness method used in this paper can also be applied to the forced vibration analyses of the steel-concrete composite beams.

References

Adam, C., Heuer, R. and Jeschko, A. (1997), "Flexural vibrations of elastic composite beams with interlayer slip", *Acta Mech.*, **125**(1), 17-30.

Banerjee, J.R. (1997), "Dynamic stiffness formulation for structural elements: a general approach", *Comput. Struct.*, **63**(1), 101-103.

Berczynski, S. and Wroblewski, T. (2005), "Vibration of steel-concrete composite beams using the Timoshenko beam model", *J. Vib. Control*, **11**(6), 829-848.

Berczynski, S. and Wroblewski, T. (2010), "Experimental verification of natural vibration models of steel-concrete composite beams", *J. Vib. Control*, **16**(14), 2057-2081.

Biscontin, G., Morassi, A. and Wendel, P. (2000), "Vibrations of steel-concrete composite beams", *J. Vib. Control*, **6**(5), 691-714.

Dilena, M. and Morassi, A. (2003), "A damage analysis of steel-concrete composite beams via dynamic methods: Part II Analytical models and damage detection", *J. Vib. Control*, **9**(5), 529-565.

Dilena, M. and Morassi, A. (2009), "Vibrations of steel-concrete composite beams with partially degraded connection and applications to damage detection", *J. Sound Vib.*, **320**(1-2), 101-124.

Girhammar, U.A. and Pan, D. (1993), "Dynamic analysis of composite members with interlayer slip", *Int. J.*

Solids Struct., **30**(6), 797-823.

Girhammar, U.A., Pan, D.H. and Gustafsson, A. (2009), "Exact dynamic analysis of composite beams with partial interaction", *Int. J. Mech. Sci.*, **51**(8), 565-582.

Lenci, S. and Clementi, F. (2012), "Effects of shear stiffness, rotatory and axial inertia, and interface stiffness on free vibrations of a two-layer beam", *J. Sound Vib.*, **331**(24), 5247-5267.

Luo, Y., Li, A. and Kang, Z. (2012), "Parametric study of bonded steel-concrete composite beams by using finite element analysis", *Eng. Struct.*, **34**, 40-51.

Morassi, A. and Rocchetto, L. (2003), "A damage analysis of steel-concrete composite beams via dynamic methods: Part I Experimental results", *J. Vib. Control*, **9**(5), 507-527.

Ranzi, G. and Bradford, M.A. (2007), "Direct stiffness analysis of a composite beam-column element with partial interaction", *Comput. Struct.*, **85**(15-16), 1206-1214.

Shen, X.D., Chen, W.Q., Wu, Y.F. and Xu, R.Q. (2011), "Dynamic analysis of partial-interaction composite beams", *Compos. Sci. Technol.*, **71**(10), 1286-1294.

Wang, Y.C. (1998), "Deflection of steel-concrete composite beams with partial shear interaction", *J. Struct. Eng.*, **124**(10), 1159-1165.

Wittrick, W.H. and Williams, F.W. (1971), "A general algorithm for computing natural frequencies of elastic structures", *Q. J. Mech. Appl. Math.*, **24**(3), 263-284.

Wolfram, S. (1991), *Mathematica: A System for Doing Mathematics by Computer*, Addison-Wesley, MA, USA.

Wu, Y.F., Xu, R. and Chen, W. (2007), "Free vibrations of the partial-interaction composite members with axial force", *J. Sound Vib.*, **299**(4-5), 1074-1093.

Xu, R. and Wu, Y. (2007), "Static, dynamic, and buckling analysis of partial interaction composite members using Timoshenko's beam theory", *Int. J. Mech. Sci.*, **49**(10), 1139-1155.

Xu, R.Q. and Wu, Y.F. (2008), "Free vibration and buckling of composite beams with interlayer slip by two-dimensional theory", *J. Sound Vib.*, **313**(3-6), 875-890.

CC